A Study on the Application Performance of High-Aspect-Ratio Nano-Ettringite in Photocurable Resin Composites

Weihua Cao * and Hong Zhu

Posted Date: 17 April 2024

doi: 10.20944/preprints202404.1163.v1

Keywords: nano-ettringite; photocurable resin; viscosity; shrinkage; tensile strength

 doi:10.20944/preprints202404.1163.v1

Article

A Study on the Application Performance of High-Aspect-Ratio Nano-Ettringite in Photocurable Resin Composites

Weihua Cao * and Hong Zhu

School of Materials Science and Engineering, Nanjing Tech University, Nanjing, Jiangsu 211800, China; whcao999@qq.com
* Correspondence: whcao999@qq.com (W.C.)

Abstract: In this study, the impact of the addition of high-aspect-ratio nano-ettringite to photocurable epoxy acrylate resin was explored, with a specific focus on the changes observed in viscosity, shrinkage, tensile strength, and elongation at the break of composites formed. Herein, the nano-ettringite samples were modified using KH-570. The 3 wt% or 6 wt% KH-570-modified and unmodified nano-ettringite were dispersed into the resin by ultrasonic treatment in conjunction with mechanical stirring. The grafting effects of nano-ettringite onto KH-570 were analyzed through scanning electron microscopy (SEM), X-ray diffraction (XRD), thermogravimetric (TG) analysis, and Fourier transform infrared spectroscopy (FTIR). The results demonstrate that increased dosages of unmodified and modified nano-ettringite led to increased viscosity of the composite while reducing shrinkage. At the same dosage, the photocurable resin with modified nano-ettringite demonstrated a lower shrinkage and a higher tensile strength. Notably, when the amount of modified nano-ettringite was 3 wt%, the highest tensile strength of the composite was 64.61 MPa, presenting a 72.57% increase compared to the blank sample. Furthermore, the incorporation of modified nano-ettringite as a filler provides a new perspective for improving the performance of photocurable epoxy acrylate resin composites.

Keywords: nano-ettringite; photocurable resin; viscosity; shrinkage;tensile strength

1. Introduction

Photocurable resin materials include epoxy resin, phenolic resin, and acrylic resin, which offer a major advantage with their rapid curing under ultraviolet (UV) radiation. However, resins are susceptible to warping and deformation during the process of light curing, generally resulting in low strength after curing. These two disadvantages of photocurable resin severely hinder the rapid development of light-curing three-dimensional (3D) printing devices in the industrial field [1,2]. To address these two drawbacks, materials with strengthening features are added for the preparation of photocurable resin composites with directional properties. The incorporation of materials with strengthening features can fully leverage the synergistic effect of two or more materials, thereby reducing the shrinkage and enhancing the tensile strength of photocurable resin composites [3–5].

As reported by numerous researchers, high-aspect-ratio materials possess high specific modulus and specific strength, which substantially enhances mechanical strength when combined with photocurable resin to form composites [6–8]. He et al. [9] synthesized a composite material by adding glass fiber as the reinforcing phase to epoxy resin for light-curing rapid prototyping, demonstrating that increasing the glass fiber content in the system led to an improvement in the shear, bending, and tensile strengths of the resin. Liu et al. [10] coated calcium sulfate whiskers (CSWs) by initially using chitosan and subsequently modifying them with acryloyl chloride to form carbon-carbon double bonds on the surface. The modified CSWs were subsequently added to the photosensitive resin. The results revealed that the incorporation of 5 wt% CSWs into the photosensitive resin increased both

 doi:10.20944/preprints202404.1163.v1

the tensile strength and impact strength by approximately 20% and 7%, respectively. Furthermore, the printed products exhibited high dimension stability and accuracy.

Generally, ettringite exhibits a needle-like or fibrous morphology and a high aspect ratio. Moreover, its raw materials are cost-effective and easy to obtain. Ettringite is often mentioned in studies related to the strength development of cement-based materials, and most studies have demonstrated that ettringite is the primary source of the early strength development of cement [11,12]. Additionally, ettringite can exhibit different morphologies in cement hydration products, such as short columns, needles, and long rods, depending on the growth environment. Among these, the high-aspect-ratio ettringite has the most significant effect on improving the cement strength [13]. Li Haiyan et al. [14] added 4 wt% ultrafine ettringite to a sulfoaluminate cement-based material to effectively produce more high-aspect-ratio ettringite materials in cement hydration products compared with the control without ettringite. This approach led to an increase in the compressive strength by 380% after 4 hours and shortened the initial setting time by 55.6%. Currently, the applications of ettringite are mostly focused on improving the strength of cement-based materials, with relatively fewer studies on the influence of ettringite on the mechanical properties of other composites.

In this study, high-aspect-ratio nano-ettringite was silanized using KH-570, thereby providing a surface with photopolymerization functional groups. The silanized nano-ettringite was subsequently dispersed into epoxy acrylic resin to prepare resin composites. Moreover, in this study, the impact of silanized and untreated nano-ettringite on the viscosity, shrinkage, tensile strength, and elongation at break of photocurable resin composites was examined. These results can promote further exploration to expand the application range of high-aspect-ratio nano-ettringite as a reinforcing material.

2. Experiment

2.1. Materials

In this study, the materials utilized are γ-methacryloxypropyl trimethoxy silane (KH-570) produced by Sinopharm Chemical Reagent Co., Ltd.; epoxy acrylic resin (4210) produced by Changzhou Ruisong Chemical Co., Ltd.; tripropylene glycol diacrylate (TPGDA) produced by New Land Polymer Materials Co., Ltd.; 2-hydroxy-2-methylpropiophenone (HMPP) produced by Kunshan Century Dragon Chemical Co., Ltd.; and nano-ettringite provided by the Nanomaterials Laboratory of Nanjing Tech University, as depicted in Figure (a,b). Notably, the prepared nano-ettringite exhibited a high aspect ratio.

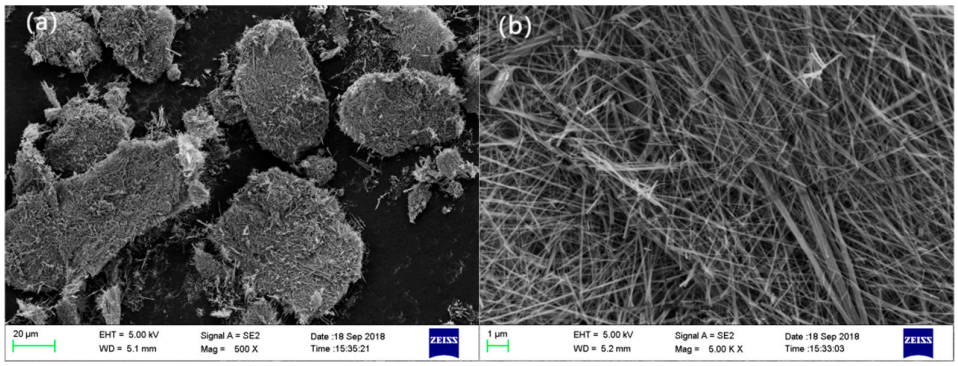

Figure 1. SEM image of nano-ettringite.

2.2. Methodology

2.2.1. Modification of Nano-Ettringite

The procedure to modify nano-ettringite is as follows: 1 g of KH-570 is added to 200 mL of ethanol solution (ethanol: water = 95:5), and the mixture is treated in ultrasound continuously for 30

 doi:10.20944/preprints202404.1163.v1

min to completely hydrolyze KH-570. Then, 4 g of nano-ettringite is weighed and added to the mixture. The mixed solution is stirred using a magnetic stirrer for 6 hours in a water bath at 45 °C. Later, the solution is filtered using a vacuum pump, and the filter cake is washed repeatedly with anhydrous ethanol and dried at 40 °C for 12 hours to obtain the KH-570-modified nano-ettringite [15,16]. Finally, the modified nano-ettringite is finely ground using a mortar, after which the powder is sealed and stored.

2.2.2. Preparation of Photocurable Resin Composites

Herein, the resin precursor solution for light-curing 3D printing is obtained by mixing epoxy acrylate resin (4210) and the active monomer (TPGDA) at a molar ratio of 1:1 for 5 hours. Then, 50 g of the resin precursor solution is weighed and 1 g of initiator is added along with nano-ettringite in mass ratios of 0%, 3%, and 6%, respectively. The mixture is stirred while dispersing them using ultrasound for 2 hours to evenly distribute nano-ettringite in the mixed solution. The evenly mixed solution is poured into the sample mold (the mold is made of glass plates and coated with Vaseline in advance), cured under UV for 10 s at a frequency of 40 kW using a light-curing device, and then removed to obtain the sample, which is displayed in Figure 2.

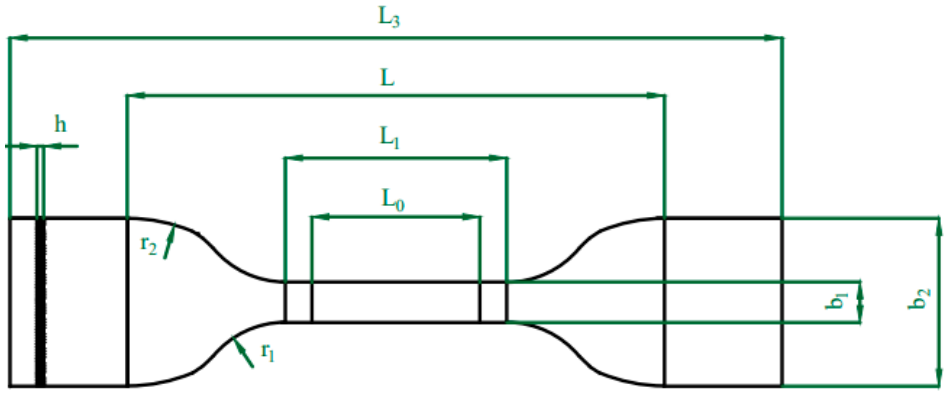

Figure 2. Tensile sample of resin.

2.3. Characterization

2.3.1. X-ray Diffraction (XRD) Analysis

Phase analysis of nano-ettringite was conducted using an X-ray diffractometer with a diffraction step of 0.5°/min, and the adopted radiation source generated Cu-Kα X-rays at 40 mA and 40 kV.

2.3.2. Fourier Transform Infrared Spectroscopy (FTIR)

To identify the nano-ettringite before and after modification, an FTIR spectrometer (Nicolet 8700, Bruker Optik GmbH, Ettlingen, Germany) was utilized with a wavenumber range of 4000–400 cm^{-1}, 32 scans, and a resolution of 4 cm^{-1}. The background spectrum was collected using a blank KBr plate.

2.3.3. Thermogravimetric (TG) Analysis

Under a nitrogen atmosphere, nano-ettringite was characterized before and after modification using a TG analyzer (TG 409PC, NETZSCH Instruments Co., Ltd., Bavaria, Germany) at a heating rate of 10 °C/min in the temperature range of 50–900 °C.

2.3.4. Viscosity Test

The viscosity of photocurable resin liquids with varying nano-ettringite contents was tested using an NDJ-79 rotary viscosimeter following the GB/T 17473.5-2008 standard.

 doi:10.20944/preprints202404.1163.v1

2.3.5. Density and Shrinkage Testing

The density of the photocurable resin liquids with various nano-ettringite contents and the density of the solidified samples were measured using an AR-120GY solid-liquid dual-purpose densimeter.

2.3.6. Mechanical Properties Testing

The mechanical properties, in particular the tensile properties and elongation at break of nano-ettringite/photocurable resin composites, were evaluated using a GX-9006 universal testing machine following the GBT1040.3-2006 standard.

Herein, resin was injected into the standard sample mold with a length of 115 mm and a width of 25 mm as specified in GBT1040.3-2006 (see Figure 2) to obtain the samples. The fixture spacing was adjusted to 25 mm, and the stretching rate was set to 50 mm/min. The tensile strength (MPa) and elongation at break were determined as per the following formulas:

The narrow, parallel section of the photocurable resin composite had a width of 6 mm and a thickness of 1 mm.

b_1—Width of the narrow parallel section: 6 mm±0.4 mm.

b_2—End width: 25 mm±1 mm.

h—Thickness: ≤1 mm.

L_0—Gauge length: 25 mm±0.25 mm.

L_1—Length of the narrow parallel section: 33 mm±2 mm.

L—Initial distance between fixtures: 80 mm±5 mm.

L_3—Total length: ≥115 mm.

r_1—Small radius: 14 mm±1 mm.

r_2—Large radius: 25 mm±2 mm.

(1) Tensile strength: $\sigma_t = \frac{P}{b \cdot h}$

b—Sample width, mm.

h—Sample thickness, mm.

P—Breaking or maximum load, N.

(2) Elongation at break: $\varepsilon_t = \frac{\Delta L_b}{L_0} \times 100$

ΔL_b—Amount of elongation within the gauge distance L_0 at the moment of sample fracture, mm.

2.3.7. Analysis of Fracture Surface Morphology

The morphological analysis of the nano-ettringite samples was conducted using a Zeiss Ultra55 produced in Germany. For the analysis, the high vacuum mode was selected, the acceleration voltage was set to 5 kV, and the sample chamber pressure was set to 1×10^{-3} Pa. Additionally, the tensile fracture surface of KH-570-modified nano-ettringite/photocurable resin was characterized, and the morphology of the cross-section was examined.

3. Results and Discussion

3.1. Infrared Analysis

In this study, the silane coupling agent KH-570 was employed that underwent Si/OH group reactions on the surface of nano-ettringite through hydrolysis to enhance the interfacial adhesion between nano-inorganic fillers and organic matrices, facilitate the dispersion of nano-inorganic fillers in organic photocurable resin, and leverage their unique size advantage. Figure 3 illustrates the infrared spectra of unmodified and modified nano-ettringite. Notably, the infrared spectrum of modified nano-ettringite revealed a -CH2- characteristic peak near 2880 cm^{-1}, a -C=O characteristic peak at 1730 cm^{-1}, and a -Si-O characteristic peak at 940 cm^{-1}. Meanwhile, it was noted that the intensity of the peak near 3400 cm^{-1}, characteristic of the -OH bond on the ettringite surface,

 doi:10.20944/preprints202404.1163.v1

weakened. These changes are indicative of the successful grafting of siloxane onto the surface of ettringite [17,18].

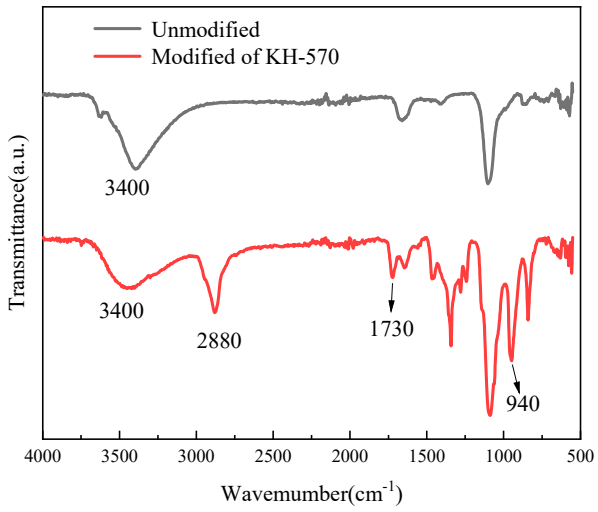

Figure 3. Infrared spectra of unmodified and modified nano-ettringite.

3.2. XRD Analysis

Figure 4 depicts the XRD analysis spectra of unmodified and modified nano-ettringite. The relative diffraction peak values reveal the presence of obvious characteristic peaks of ettringite in both spectra [19]. This suggests that no new characteristic diffraction peaks appeared in the XRD image of the modified nano-ettringite under the action of the silane coupling agent KH-570, verifying that the crystal structure of nano-ettringite encapsulated by KH-570 was unaffected.

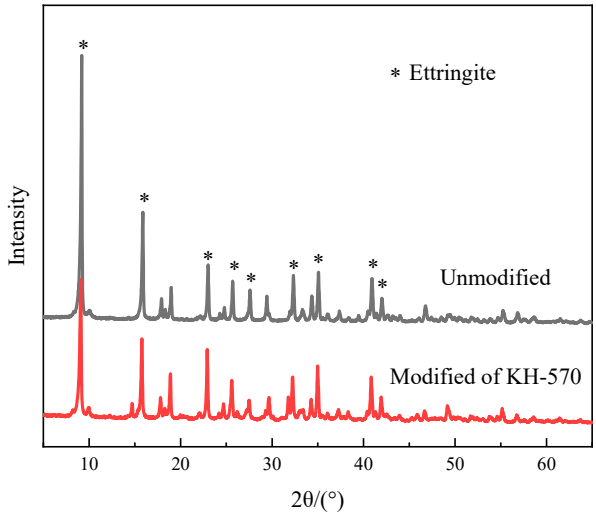

Figure 4. XRD patterns of unmodified and modified nano-ettringite.

3.3. TG Analysis

The unmodified and KH-570-modified nano-ettringite samples were heated from 50 to 900 ℃ at a heating rate of 10 ℃/min in a nitrogen atmosphere to further verify the modification effect of KH-570. Subsequently, the grafting effect of KH-570 on nano-ettringite was analyzed by comparing the thermal weight loss rates of the samples [20]. As depicted in Figure 5, unmodified nano-ettringite

 doi:10.20944/preprints202404.1163.v1

started losing weight at a temperature of 100 ℃, with a rapid increase in the loss at around 250 ℃. However, the thermal weight loss rate of the nano-ettringite modified with KH-570 was considerably slowed down, and rapid weight loss occurred until around 350 ℃. This is attributed to the improved thermal stability following coating KH-570 on the surface of nano-ettringite, making it more difficult for the modified sample to lose water under heating. Nevertheless, this evaporation of crystal water is pronounced in the structure of unmodified ettringite under heating [21]. This result confirmed the successful grafting of KH-570 onto the surface of nano-ettringite.

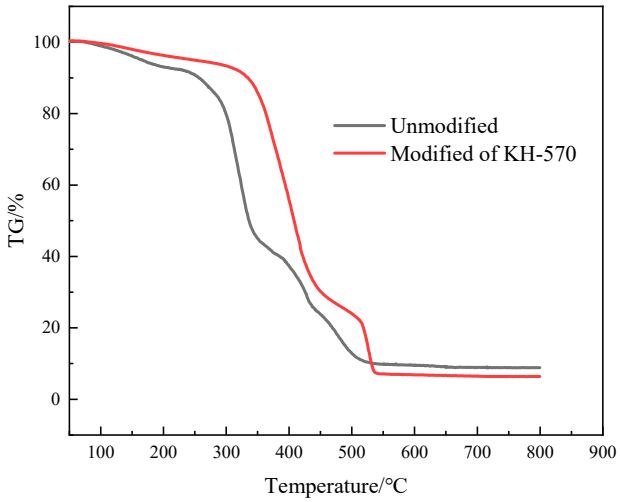

Figure 5. TG analysis graphs of unmodified and modified nano-ettringite.

3.4. Effect of Nano-Ettringite Dosage on the Viscosity of Photocurable Resin Composite Solutions

It is observed that the viscosity of photocurable resin impacts the speed of 3D printing and the accuracy of devices [22]. Hence, it is imperative to analyze the viscosity changes of composite resins. Table 1 illustrates the impact of unmodified and modified nano-ettringite dosages on the viscosity of the photocurable composite resin. Notably, the viscosity of the composite resin increased as the amount of unmodified and modified nano-ettringite increased. This is attributed to the tendency of the more high-aspect-ratio nano-ettringite particles to overlap with each other, forming an internal skeleton system [23]. Consequently, the movement of the photocurable resin becomes difficult, resulting in increased viscosity [24]. At the same dosage, the viscosity of the KH-570-modified nano-ettringite composite resin was observed to be higher compared to the unmodified nano-ettringite composite resin, with an increase of 20 mPa·s and 30 mPa·s under the respective dosages of 3 wt% and 6 wt%. This can be attributed to the better adhesion between the modified nano-ettringite and the photocurable resin interface. Conversely, the more even dispersion of the modified nano-ettringite in the photocurable resin that results in a larger amount of skeleton construction also contributed to this increase. Overall, the viscosity of the composite resin system was below 700 mPa·s, satisfying the molding requirements for light-curing 3D printing.

Table 1. Effect of unmodified and modified nano-ettringite dosages on the viscosity of photocurable resin composites.

Sample	Viscosity (mPa·s)
Pure photocurable resin	420
3wt% nano-ettringite/photocurable resin composite	540
6wt% nano-ettringite/photocurable resin composite	610
3wt% modified nano-ettringite/photocurable resin composite	560
6wt% modified nano-ettringite/photocurable resin composite	640

 doi:10.20944/preprints202404.1163.v1

3.5. Effect of Nano-Ettringite Dosage on shrinkage of Photocurable Resin

The shrinkage of photocurable resin is considered a major factor impacting 3D printing accuracy. It is observed that during the curing process of liquid resin, the van der Waals force distance between liquid molecules transitions to the covalent bond distance between solid polymer structural units, and the basic unit distance of molecules decreases, resulting in curing shrinkage [25,26]. Herein, the photocurable resin was filled with inorganic non-shrinking components of unmodified and modified nano-ettringite to compensate for the gaps caused by the shrinkage of the organic components. Table 2 presents the impact of the dosage of unmodified and modified nano-ettringite on the shrinkage of photocurable resin. Notably, the curing shrinkage of the photocurable resin composite was reduced by the addition of unmodified or modified nano-ettringite; the higher the dosage, the smaller the curing shrinkage. Furthermore, under the same dosage, the addition of modified nano-ettringite demonstrated a stronger improvement effect on the curing shrinkage of photocurable resin compared to the addition of unmodified nano-ettringite. This is due to the addition of organic groups on the surface of nano-ettringite modified with the KH-570 coupling agent, thereby enhancing the bonding ability at its interface with photocurable resin and reducing the interface gap of shrinkage polymerization of the resin molecules [27]. Furthermore, this confirmed that adding modified nano-ettringite to photocurable resin is more conducive to improving the accuracy of 3D printing materials.

Table 2. Effect of unmodified and modified nano-ettringite dosages on the shrinkage of photocurable resin composites.

Sample	Liquid density (g/cm^3)	Solid density (g/cm^3)	Shrinkage /%
Pure photocurable resin	1.1030	1.2050	8.46
3wt% nano-ettringite/photocurable resin composite	1.1140	1.2110	8.01
6wt% nano-ettringite/photocurable resin composite	1.1305	1.2242	7.65
3wt% modified nano-ettringite/photocurable resin composite	1.1188	1.2150	7.92
6wt% modified nano-ettringite/photocurable resin composite	1.1289	1.2219	7.61

3.6. Effect of Nano-Ettringite Dosage on Tensile Strength and Elongation at Break of Photocurable Resin Composites

Figure 6 depicts the tensile strength and elongation at break of photocurable resin composites with varied amounts of unmodified and modified nano-ettringite. As shown in Figure 6(a),the tensile strength of the unmodified nano-ettringite samples increased with increasing dosage. Meanwhile, the tensile strength of modified nano-ettringite samples initially increased and decreased subsequently with increasing dosage, though it remained higher compared to the blank sample. Compared to that of the unmodified nano-ettringite/photocurable resin composite, the tensile strength of the modified nano-ettringite/photocurable resin composite increased by 17.03 MPa and 9.59 MPa, respectively, at the same dosage of 3 wt% and 6 wt%. This is indicative of the higher tensile strength provided by the modified nano-ettringite for the photocurable resin composite at a smaller dosage. However, agglomeration can occur when the dosage of modified nano-ettringite is increased to a certain level, weakening its bonding strength with photocurable resin and resulting in a reduced tensile strength [28,29]. Furthermore, the elongation at the break of the samples decreased with more nano-ettringite or modified nano-ettringite in Figure 6(b). Besides, the elongation at the break of the samples with modified nano-ettringite was smaller under the same dosage. This is because high-aspect-ratio nano-ettringite can easily form a cross-linked network structure, enhancing the rigidity and reducing the elongation at break. Another reason for this is the stronger bonding ability at the modified nano-ettringite and photocurable resin interface [30].

 doi:10.20944/preprints202404.1163.v1

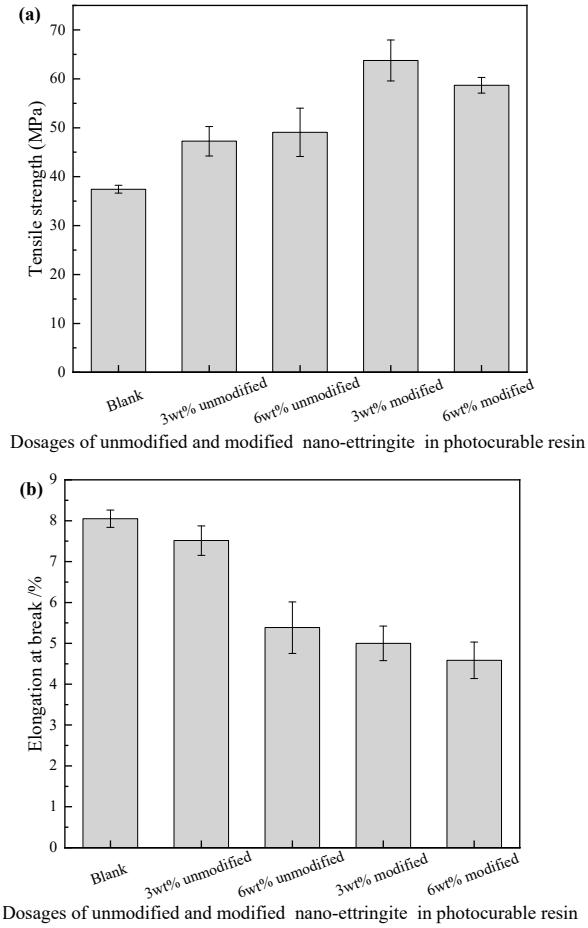

Figure 6. Effect of unmodified and modified nano-ettringite dosages on the tensile strength of photocurable resin composites.

3.7. Tensile Fracture Surface Analysis

Figure 7 illustrates the SEM images of the tensile fracture surfaces of pure photocurable resin and resin composites with 3 wt% of nano-ettringite and modified nano-ettringite. As depicted in Figure 7(a,b), the tensile fracture surface of pure photocurable resin is relatively smooth without severe uneven tearing patterns, exhibiting typical brittle fracture behavior. Figure 7(c,d) displays numerous nano-ettringite clusters, indicating poor dispersion of nano-ettringite in photocurable resin, which can easily cause stress concentration points and failure to fully utilize the advantages of nanomaterials [31]. Figure 7(e,f) exhibits the even distribution of modified nano-ettringite in photocurable resin, confirming that the nano-ettringite formed a good contact interface with photocurable resin after being modified by the KH-570 coupling agent. Consequently, their bonding was closer, which is conducive to the dispersion of modified nano-ettringite in the resin matrix, thereby avoiding the occurrence of stress concentration points. Furthermore, nano-ettringite and photocurable resin demonstrated good compatibility, as evidenced by the close connection at the interface.

 doi:10.20944/preprints202404.1163.v1

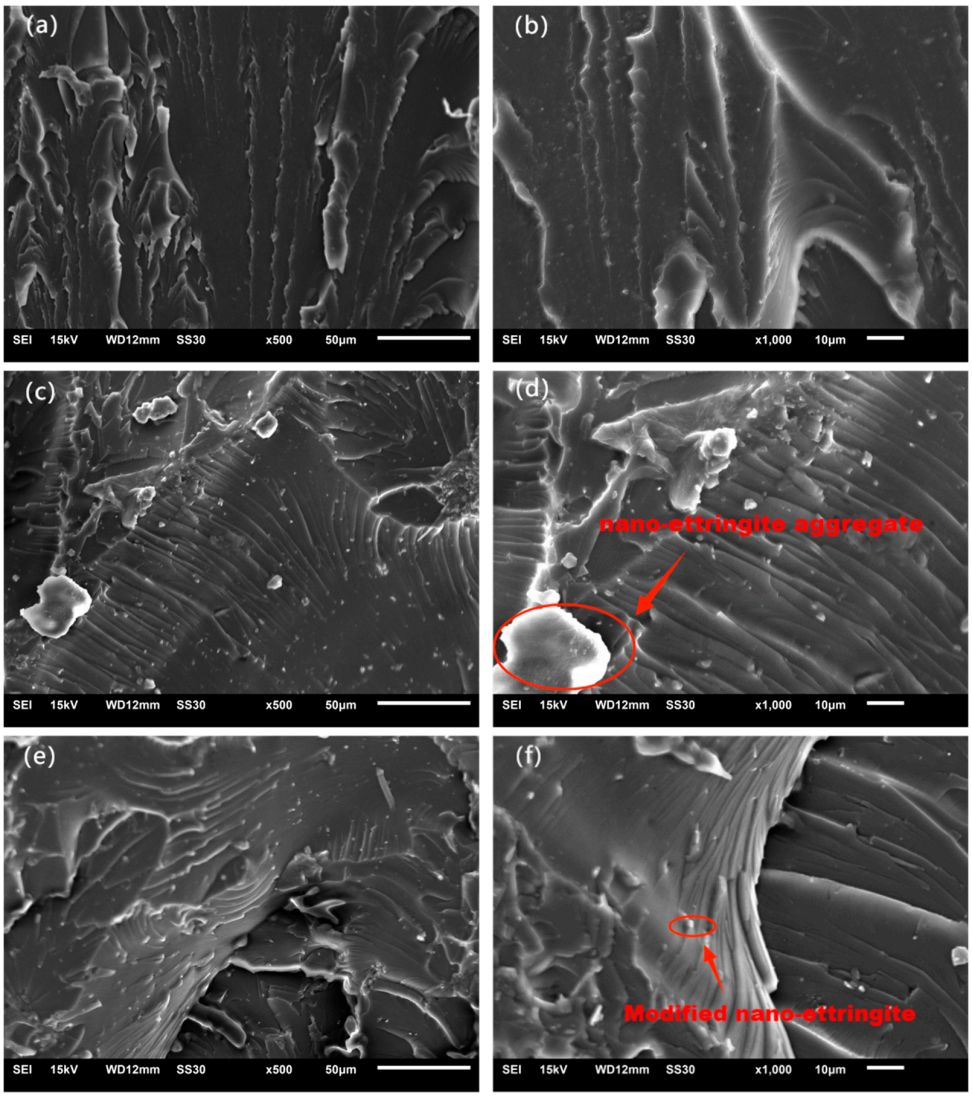

Figure 7. SEM images for tensile fracture surfaces of the photocurable resin. (**a, b**) Pure photocurable resin; (**c, d**) 3 wt% nano-ettringite/photocurable resin composite; (**e, f**) 3 wt% modified nano-ettringite/photocurable resin composite.

4. Conclusion

In conclusion, the photocurable resin composites doped with nano-ettringite or modified nano-ettringite exhibited significant improvements in tensile mechanical properties and a reduction in shrinkage. Notably, the tensile strength of the modified nano-ettringite/photocurable resin composite was higher under the same dosage. Moreover, its SEM fracture surface demonstrated a more uniform distribution of modified nano-ettringite in photocurable resin. Among the samples, the photocurable resin composite with 3 wt% modified nano-ettringite presented the highest tensile strength (64.61 MPa), which was 72.57% higher compared to pure photocurable resin. Additionally, the shrinkage of the photocurable resin composite with modified nano-ettringite was lower compared to the unmodified nano-ettringite. This can be attributed to the stronger bonding ability and smaller interface gap between modified nano-ettringite and photocurable resin. Thus, it is concluded that employing KH-570-modified nano-ettringite with an appropriate weight ratio as the filler proved effective in improving the tensile strength and reducing the shrinkage of photocurable resin.

Author Contributions: For research articles with several authors, a short paragraph specifying their individual contributions must be provided. The following statements should be used “Conceptualization, W.C. and H.Z.;

methodology, H.Z.; software, W.C.; validation, W.C. and H.Z.; formal analysis, W.C. and H.Z.; investigation, W.C.; resources, H.Z.; data curation, W.C.; writing—original draft preparation, W.C.; writing—review and editing, W.C.; visualization, H.Z; supervision,H.Z.; project administration, H.Z; funding acquisition, H.Z. All authors have read and agreed to the published version of the manuscript.

Funding: This work was supported by Priority Academic Program Development (PAPD) of Jiangsu Higher Education Institutions.

Institutional Review Board Statement: Not applicable.

Informed Consent Statement: Not applicable.

Data Availability Statement: Data are contained within the article and Supplementary Materials.

Conflicts of Interest: The authors declare no conflicts of interest.

References

1. Zong, X.W.; Hu, Q.Y.; Wang, X. *Rapid casting technology for complex parts by UV cured 3D printing*; Huazhong University of Science and Technology Press: Wuhan, China, 2019.
2. Zong, X.W.; Hu, Q.Y.; Wang, X. *Rapid casting technology of complex parts for light curing 3D printing*; Huazhong University of Science and Technology Press: Wuhan, China, 2019.
3. Alhawiatan, A.S.; Alqutaym, O.S.; Aldawsari, S.N.; Zuhair, F.A.; Alqahtani, R.O.; Alshehri, T.H. Evaluation of silver nanoparticles incorporated acrylic light cure resin trays. *J. Pharm. Bioallied. Sci.* **2020**, *12*, S173-s175, doi:10.4103/jpbs.JPBS_52_20.
4. Ide, K.; Nakajima, M.; Hayashi, J.; Hosaka, K.; Ikeda, M.; Shimada, Y.; Foxton, R.M.; Sumi, Y.; Tagami, J. Effect of light-curing time on light-cure/post-cure volumetric polymerization shrinkage and regional ultimate tensile strength at different depths of bulk-fill resin composites. *Dent. Mater. J.* **2019**, *38*, 621-629, doi:10.4012/dmj.2018-279.
5. Medikasari, M.; Herda, E.; Irawan, B. Effect of resin thickness and light-curing distance on the diametral tensile strength of short fibre-reinforced resin Composite. *J. Phys.: Conf. Ser.* **2018**, *1073*, 052015, doi:10.1088/1742-6596/1073/5/052015.
6. Hu, X.; Liu, M.; Ji, Y.; Du, Y.; Wang, L.; Zhou, X.; Zhang, F. Enhanced mechanical properties and biosafety evaluation of surface-modified fiberglass-reinforced resin-based composite piles. *J. Mater. Sci. Mater. Med.* **2019**, *30*, 70, doi:10.1007/s10856-019-6269-z.
7. Bi, Y.Y.; Driscoll, M.S.; Meyer, R.W.; Larsen, L.S. Visible light curing of fiberglass-reinforced ballistic panels based on epoxy acrylate resin. *RadTech Rep.* **2016**, *2*, 50-53.
8. dos Santos, M.N.; Opelt, C.V.; Lafratta, F.H.; Lepienski, C.M.; Pezzin, S.H.; Coelho, L.A.F. Thermal and mechanical properties of a nanocomposite of a photocurable epoxy-acrylate resin and multiwalled carbon nanotubes. *Mater. Sci. Eng. A* **2011**, *528*, 4318-4324, doi:10.1016/j.msea.2011.02.036.
9. He, F.; Wang, Y.L.; Huang, Y.; Wan, Y.Z. Preparation and mechanical properties of 3-D braided glass fiber reinforced light-cured resin composites. *Mater. Lett.* **2006**, *60*, 3339-3341, doi:10.1016/j.matlet.2006.03.014.
10. Liu, Y.; Lin, Y.; Jiao, T.; Lu, G.; Liu, J. Photocurable modification of inorganic fillers and their application in photopolymers for 3D printing. *Polym. Chem.* **2019**, *10*, 6350-6359, doi:10.1039/C9PY01445D.
11. Fu, B. Effect of ettringite expansion agent on mechanical properties of cement-based materials. *Jilin Transportation Science and Technology* **2022**, 10-12.
12. Guo, J. Preparation of ettringite whisker and its strengthening and toughening effect on cement and gypsum. Master thesis, Hebei University of Technology, Hebei, 2020.
13. Li, Y.; Qiao, X. Effects of external factors on crystal structure and morphology of ettringite. *Bull. Silicate* **2019**, *42*, 31-47, doi:10.16552/j.cnki.issn1001-1625.20221118.004.
14. Li, H.; Guan, X.; Zhang, X.; Ge, P.; Hu, X.; Zou, D. Influence of superfine ettringite on the properties of sulphoaluminate cement-based grouting materials. *Constr. Build. Mater.* **2018**, *166*, 723-731, doi:10.1016/j.conbuildmat.2018.02.013.
15. Wang, L.; Li, R.; Wang, C.; Hao, B.; Shao, J. Surface grafting modification of titanium dioxide by silane coupler KH570 and its influences on the application of blue light curing ink. *Dyes Pigments* **2019**, *163*, 232-237, doi:10.1016/j.dyepig.2018.11.048.
16. Liu, L.; Liu, X.; Chen, J.; Zhao, X. Feasibility study on preparation of flame retardants from ettringite. *Guangdong Build. Mater.* **2022**, *38*, 16-17, doi:10.3969/j.issn.1009-4806.2022.07.007.
17. Chen, L.; Wang, Y.; Zia Ud, D.; Fei, P.; Jin, W.; Xiong, H.; Wang, Z. Enhancing the performance of starch-based wood adhesive by silane coupling agent(KH570). *Int. J. Biol. Macromol.* **2017**, *104*, 137-144, doi:10.1016/j.ijbiomac.2017.05.182.
18. Zhou, Y.; Yu, J.; Wang, X.; Wang, Y.; Zhu, J.; Hu, Z. Preparation of KH570-SiO_2 and their modification on the MF/PVA composite membrane. *Fibers Polym.* **2015**, *16*, 1772-1780, doi:10.1007/s12221-015-5284-z.

 doi:10.20944/preprints202404.1163.v1

19. Goetz-Neunhoeffer, F.; Neubauer, J.; Schwesig, P. Mineralogical characteristics of Ettringites synthesized from solutions and suspensions. *Cement Concrete Res.* **2006**, *36*, 65-70, doi:10.1016/j.cemconres.2004.04.037.
20. Guimarães, D.; de A. Oliveira, V.; Leao, V.A. Kinetic and thermal decomposition of ettringite synthesized from aqueous solutions. *J. Therm. Anal. Calorimetry* **2016**, *124*, 1679-1689, doi:10.1007/s10973-016-5259-3.
21. Dweck, J.; Ferreira da Silva, P.F.; Büchler, P.M.; Cartledge, F.K. Study by thermogravimetry of the evolution of Ettringite phase during type II Portland cement hydration. *J. Therm. Anal. Calorimetry* **2002**, *69*, 179-186, doi:10.1023/A:1019950126184.
22. Quan, H.; Zhang, T.; Xu, H.; Luo, S.; Nie, J.; Zhu, X. Photo-curing 3D printing technique and its challenges. *Bioact. Mater.* **2020**, *5*, 110-115, doi:10.1016/j.bioactmat.2019.12.003.
23. Chen, C.T.; Struble, L.J. Cement–dispersant incompatibility due to ettringite bridging. *J. Am. Ceram. Soc.* **2011**, *94*, 200-208, doi:10.1111/j.1551-2916.2010.04030.x.
24. Gojzewski, H.; Sadej, M.; Andrzejewska, E.; Kokowska, M. Dataset for acrylate/silica nanoparticles formulations and photocured composites: Viscosity, filler dispersion and bulk Poisson′ s ratio. *Data Brief* **2017**, *12*, 528-534, doi:10.1016/j.dib.2017.04.040.
25. Charton, C.; Colon, P.; Pla, F. Shrinkage stress in light-cured composite resins: influence of material and photoactivation mode. *Dent. Mater.* **2007**, *23*, 911-920, doi:10.1016/j.dental.2006.06.034.
26. Fang, H.; Guymon, C.A. Recent advances to decrease shrinkage stress and enhance mechanical properties in free radical polymerization: A review. *Polym. Int.* **2022**, *71*, 596-607, doi:10.1002/pi.6341.
27. Mallakpour, S.; Madani, M. The effect of the coupling agents KH550 and KH570 on the nanostructure and interfacial interaction of zinc oxide/chiral poly (amide–imide) nanocomposites containing l-leucine amino acid moieties. *J. Mater. Sci.* **2014**, *49*, 5112-5118, doi:10.1007/s10853-014-8220-5.
28. Ashraf, M.A.; Peng, W.; Zare, Y.; Rhee, K.Y. Effects of size and aggregation/agglomeration of nanoparticles on the interfacial/interphase properties and tensile strength of polymer nanocomposites. *Nanoscale Res. Lett.* **2018**, *13*, 214, doi:10.1186/s11671-018-2624-0.
29. Bhuiyan, M.; Kalaitzidou, K.; Georgia Institute of Technology; Karevan, M.; Georgia Tech. Understanding effects of interfacial contact and agglomeration of fillers on tensile modulus of polymer nanocomposites. In Proceedings of the 69th Annual Technical Conference of the Society of Plastics Engineers 2011 (ANTEC 2011), Boston, MA, United States, 1-5 May, 2011; pp. 802-807.
30. Ghasemi, F.A.; Niyaraki, M.N.; Ghasemi, I.; Daneshpayeh, S. Predicting the tensile strength and elongation at break of PP/graphene/glass fiber/EPDM nanocomposites using response surface methodology. *Mech. Adv. Mater. Struct.* **2021**, *28*, 981-989, doi:10.1080/15376494.2019.1614702.
31. Satterthwaite, J.D.; Maisuria, A.; Vogel, K.; Watts, D.C. Effect of resin-composite filler particle size and shape on shrinkage-stress. *Dent. Mater.* **2012**, *28*, 609-614, doi:10.1016/j.dental.2012.01.007.